



Vertical Electron Density Profile Estimation using Ground based Ionosonde and in-situ Density Measurement over Dibrugarh

B. R. Kalita^{***} and P.K. Bhuyan^{*}

^{*}Centre for Atmospheric Studies, Dibrugarh University, Rajabheta, Dibrugarh, Assam, India.

^{**}Department of Physics, Dibrugarh University, Rajabheta, Dibrugarh, (Assam), INDIA

(Corresponding author: B. R. Kalita)

(Received 23 November, 2017 accepted 12 December, 2017)

(Published by Research Trend, Website: www.researchtrend.net)

ABSTRACT: In this paper we report the results of bottom side electron density measurement carried out in the low latitude station of Dibrugarh (27.5° N, 94.9° E, DIP 43°N). The bottom side electron density of the ionosphere over Dibrugarh is measured using a Canadian Advanced Digital Ionosonde (CADI). The bottomside profile is obtained from the real height inversion of the CADI ionograms using the profile inversion software POLAN. The topside density profile is estimated by fitting the ROCSAT-1 in situ electron density measurement to a α -Chapman profile. The results of the topside fitting to the satellite data is the topside scale height. The topside vertical density profile is then reconstructed with the “effective scale height”. Total vertical electron density profile over this location is constructed by adding the bottom side obtained from POLAN and topside obtained from the Chapman profile fitting. The reconstructed vertical electron density profile is validated by and compared with the IRI2012 predicted profile which shows significant differences at day time but similarity in the morning and night time.

Keyword: Ionosphere; density profile; scale height.

I. INTRODUCTION

The spatial distribution of the electron density in the ionosphere is of considerable scientific importance. In addition to practical applications like time delay correction of GPS signals, vertical electron distribution profile is the key to many scientific research areas like empirical modeling of the ionosphere. Ground based ionosonde is still the basic tool for studying the bottom side electron density distribution (Rishbeth and Garriot, 1969). The ionospheric density profile measured up to the F layer peak using ionosonde is defined as bottom side and is widely available due to global network of ionosondes. But the part of the density profile above the F layer is not accessible to the ionosondes and can be measured only by Incoherent Scatter Radar (ISR) or Topside sounders aboard satellites. The (ISR) facility is sparse due to the cost involved. The topside sounder data is available only for a limited time period as there has been no current satellites mission carrying any topside sounder. Therefore, the knowledge about the density profile of the topside ionosphere remains poor. To overcome this limitation, many innovative techniques have been applied to estimate the topside density, e.g., method based on radio occultation observation on board low earth orbiting satellites like CHAMP and COSMIC (Stankov 2006, Libo Liu 2008). Analytical Modeling using mathematical functions like

exponential, parabolic, Epstein and Chapman functions etc have been done to estimate the topside profile (e.g. Booker, 1977; Rawer *et al.*, 1985; Rawer, 1988; Di Giovanni and Radicella, 1990; Stankov *et al.*, 2003). All these functions describe the variation of electron density in terms of a quantity called Scale height. This important quantity is basically a proxy for the plasma scale height and, therefore, it has dimensions of length. Plasma scale height is defined (Davies, 1990; Hargreaves, 1992) as $H_p = kT_p/mg$, where m is the ion mass, $T_p = (T_i + T_e)/2$ is the plasma temperature, T_i and T_e are ion and electron temperatures, k is the Boltzmann constant (1.380658×10^{-23} J/deg). Scale height defines the shape of the electron density profile and is an indicator of the thickness of the profile.

In practice, the vertical scale height can be approximately deduced as the vertical distance in which the electron concentration changes by a factor of an exponent e . The value of the scale height indicates the gradient of the electron density (Stankov 2005). Therefore study of the scale height is very important as it may lead to understanding of physics related to the ion composition and dynamics of the upper ionosphere (Stankov, 2005; Hanson and Ortenburger, 1961; Horwitz *et al.*, 1990).

The α -Chapman function representation of the density profile is a useful and realistic approach.

The Chapman function is simple and has great potential for analytical modeling of the ionospheric profile (e.g. Huang and Reinisch, 2001). It has been reported that (Reinisch and Huang, 2004; Belehaki *et al.*, 2003) the Chapman function, even with a constant scale height, fits the topside ionospheric profile well up to several hundred kilometers above the F2-peak. Therefore a new approach was introduced by Reinisch and Huang (2001) and Huang and Reinisch (2001) where they tried to use bottom side ionosonde data to extrapolate the topside density variation. They used the approximation that the scale height above the peak of the F2 layer is constant and equal to the Chapman scale height at the height of F2 layer peak density ($hmF2$). Using this constant scale height the topside profile was reconstructed. Since this method uses only bottom side information and with no information from the top side, the derived profiles are unlikely to match the true profile very closely. Tulasi Ram *et al.* (2009) have introduced an advanced method where the satellite (ROCSAT-1) in situ density measurements are assimilated with ionosonde measurements to determine the topside effective scale height (H_T) using an α -Chapman function over the equatorial location, Jicamarca. Venkatesh *et al.* (2011) have also applied this method for the equatorial station of Trivandrum (8.47°N, 76.91° E) and low latitude station of Waltair (17.7°N, 83.3° E) in the Indian region. To further add to these knowledge base, a similar approach have been applied in this paper by using data from ROCSAT -1 satellite in situ measurements over the low latitude station of Dibrugarh (27.5°N, 94.9°E, dip 23°N) which is at the outer slope of the northern equatorial anomaly region. The ROCSAT-1 is for the falling solar activity period of 1999 to 2004 of solar cycle 23. We estimate the topside profile using the “effective constant scale height” method (Tulasi Ram *et al.*, 2009) and then compare the profile with IRI 2012 predicted density profile.

II. DATA AND METHODOLOGY

The data used in this paper are the bottom side measurements of CADI for the period of July 2010 till January 2013 and the in situ electron density measurements made by ROCSAT-1 satellite (www.cdaweb.com) from 2000 till 2004 over Dibrugarh (27.5°N, 94.9°E).

We have based our study on the assumption that on two days when the solar flux is same and geomagnetic activity are similar; the electron density at heights far above the F2 layer peak will be same or similar. Borgohain and Bhuyan (2010) have reported that the ion density measured by SROSS C2 and FORMOSAT-1 (ROCSAT-1) are positively correlated with $F_{10.7}$ both during day time and night time.

It is also reported (Rich *et al.*, 2003) that the variations in electron density correlate better with $F_{10.7}$ at altitude far above the F2 layer peak. Therefore, we have assumed that the ion density at the heights of 600km of ROCSAT-1 satellite measurement are similar for two days of similar solar flux and geomagnetic activity. Based on this conjecture, a geo-magnetically quiet day (<http://wdc.kugi.kyoto-u.ac.jp/qddays/index.html> and $Kp < 3$) is selected from the period August 2010 till January 2013 on which the average solar flux ($F_{10.7p}$) is same as that of a day of the same month from the period 1995-2004 where ROCSAT-1 in situ measurements of density over Dibrugarh are available. Instead of daily $F_{10.7}$, we have used the average of daily $F_{10.7d}$ and the average of 81-days $F_{10.7}$ centered on that day called $F_{10.7p}$. This way we have an approximate value of the electron density at 600km for the date when CADI measurements are available. CADI ionograms for that date is then scaled using POLAN (Titheridge, 1985) to obtain the bottom side electron density profile, peak value of the F2 layer electron density $NmF2$ and the height of F2 layer peak density $hmF2$.

Values of $NmF2$, $hmF2$ and the ROCSAT-1 measured in situ density at 600 km (h_s) is fitted into the Chapman function-

$$N(h) = NmF2 \cdot \exp[1/2(1 - z - \exp^{-z})] \quad \dots(1)$$

$$\text{where } z = (h - hmF2)/H_T \quad \dots(2)$$

and H_T the Chapman scale height.

The initially unknown value of scale height H_T is adjusted iteratively till the difference between $N(h_s)$ and the satellite in situ measurement is the least. The value of H_T at the end of this fitting process is assumed to be the effective scale height of the topside density profile. This process is explained in Fig. 1 (a) and Fig 1(b). The black line in the Fig 1(a) represents the bottom side electron density derived from CADI ionogram using POLAN at 1400 hrs LT on 11 August 2012. The star indicates the ROCSAT-1 measured in situ electron density ($1.31 \times 10^{12} / m^3$) at an altitude of 600.5 km. The α -Chapman function (Eq. 1) is fitted between the two points -F2-layer peak density marked by the red arrow in Fig. 1(b) and ROCSAT-1 in situ density marked by black arrow to obtain the previously unknown scale height value H_T . The value of H_T (42 km) is then used in the α -Chapman function (Eq. 1) to reconstruct the topside profile from $hmF2$ to 1000km as shown in Fig. 1(b).

The total electron density profile is then obtained by adding the POLAN bottom side profile and this reconstructed topside profile. The F2 layer critical frequency $foF2$ and real height of the F2 layer peak $hmF2$ varies on days of same solar activity.

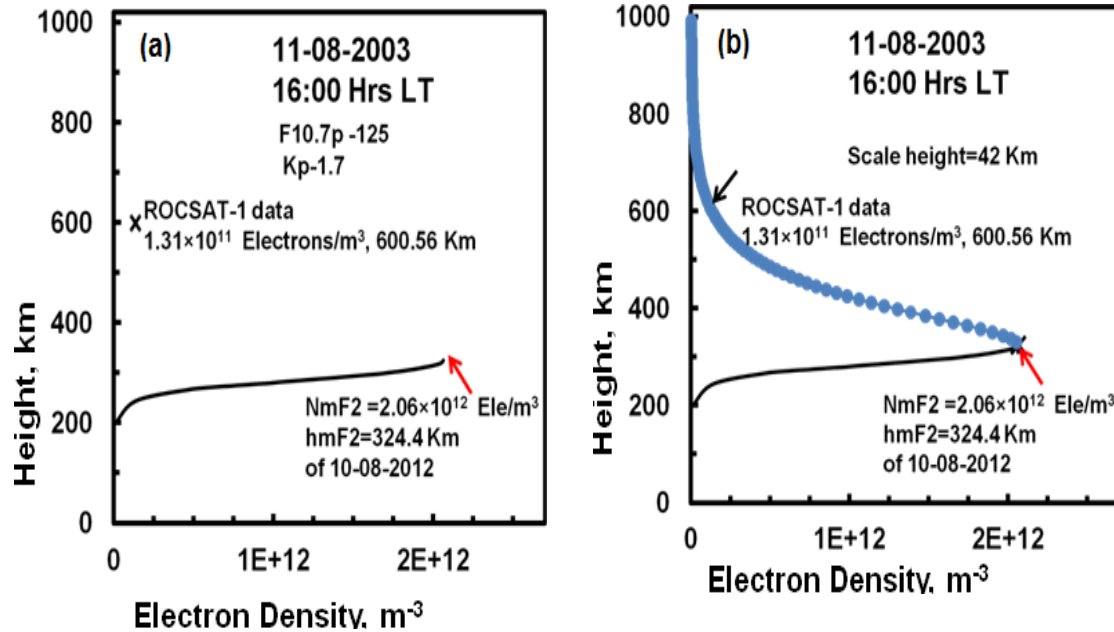


Fig. 1. (a) The Bottom side profile obtained from CADI ionogram on 10-08-2012 at 1600 hrs LT over Dibrugarh (b) fitting α -Chapman function between F2 layer peak and ROCSAT in situ measurement made on 11-08-2003 at 1600 hrs LT.

Therefore, this process is then repeated for all the available satellite data points at different hours of the day and for different seasons of the year. The ionosonde data is filtered to reject magnetically disturbed days as well as two days post disturbance.

To estimate the error that might have been introduced in the process described above, we make the following study. In the first study, we calculate the variations in the estimated scale height for the same solar flux and geomagnetic conditions. This gives a maximum variation of about 12% in the value of H_T . In the second study, taking into consideration the possible error in the bottom side ionogram inversion process of POLAN, we change the height of peak electron density, $hmF2$ as obtained from the bottom side POLAN profile by ± 10 km and repeat the fitting process. The resultant H_T value shows a variation of less than 10%. For each satellite data point, three ionograms around the time of satellite measurement is analyzed and their variability is calculated. During the sunrise period of 0500-0600 hrs LT, significant variation in scale height values are observed for the three ionograms. The profiles obtained with this method are compared with the vertical electron density profiles for the same selected days predicted by the IRI 2012 model (http://omniweb.gsfc.nasa.gov/vitmo/iri2012_vitmo.html) up-to 1000 km.

III. RESULTS AND DISCUSSION

A. Diurnal variation of estimated vertical electron density profile

Vertical electron density profiles over Dibrugarh are estimated for different local times of the day where ROCSAT-1 data are available. In Fig. 2, diurnal variation of the reconstructed vertical density profile over Dibrugarh is shown for one sample day. Due to constrain of data availability, these profiles were obtained over a period covering low to moderate solar activity. The bottom side ionograms are available for every 15 or 20 minutes. Therefore maximum possible difference between bottom side profile and topside satellite data can be 10 minutes but we considered only those satellite data where the difference is less than 5 minutes. We note that the peak density ($NmF2$) is around 300 km during midnight and the topside is thicker than the bottom side. The peak density decreases in the post midnight period and the topside thickness also increases. This is expected as recombination at the bottom side reduces the density and the topside is supplemented by small plasmaspheric diffusion. The bottom side starts to grow during sunrise and the total profile is thickest during this period although peak density and total electron content is very low.

The height of the peak density (hmF_2) is maximum during dawn or pre-sunrise period (04-06 LT) and decreases as density build up in the bottom side due to solar production thereafter. The layer stratification is observed during 08-09 LT with formation of F1 layer. The height of the layer (hmF_2) jumps suddenly during 10LT and reaching 400Km or more. This could be due to the increase in the vertical $E \times B$ drift during this period which pushes the plasma upwards in the low latitude region. The highest F2 layer is observed during 11-12 LT coinciding with the peak in vertical drift (Scherliess and Fejer, 1983). The layer density saturates during 12-16 LT with minimum change in height or density. The topside is thicker during 15-16 LT due plasma transport from the equatorial fountain effect (Borghain and Bhuyan, 2010). The bottom side begins to shrink in the post sunset (17 LT-) period as the solar radiation is reduced and eventually production ceases. Plasma is lost quickly due to recombination.

During the pre-midnight period the density slowly decreases and the layer moves up slightly due to equator ward meridional winds which pushes the plasma up along the field lines. The diurnal variation is evidently controlled by equatorial vertical plasma drift as the height of maximum density hmF_2 peaks in the same time period. The maximum density of the layer is around 15-16 LT which corresponds to the development of equatorial ionization anomaly in the low latitude region. The vertical density distribution is validated by comparing with IRI 2012 model. IRI 2012 is run with bottom side thickness option ABT 2009 and topside with Nequick. CCIR is used as foF2 model. The IRI model is able to reproduce the observed profile only during a very limited period of time. The model estimated the measured distribution reasonably well during 03-06 LT and 20-22 LT. The model slightly underestimated both NmF_2 and hmF_2 during pre-midnight period.

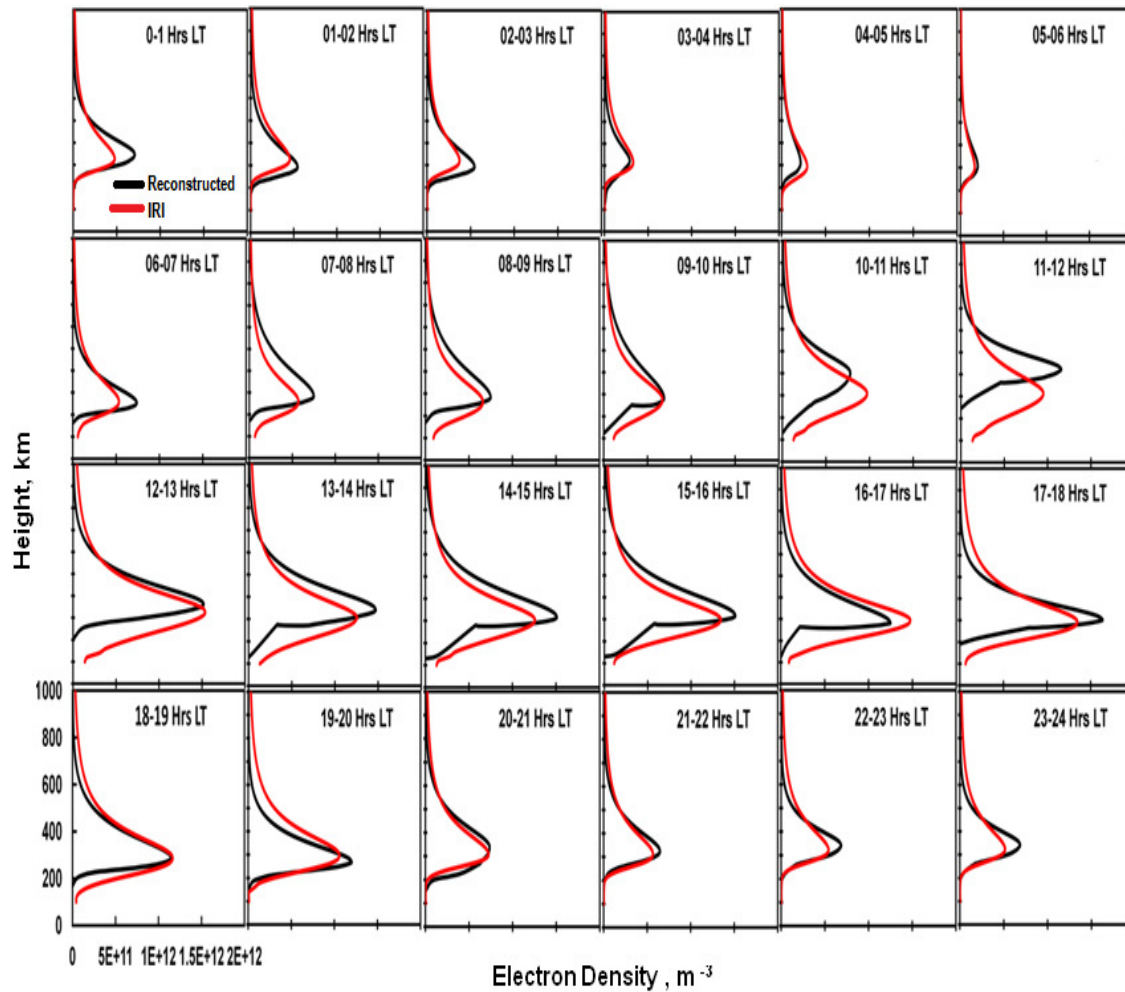


Fig. 2. Diurnal variation of reconstructed vertical electron density profiles and the comparison with IRI predicted profiles.

For other times of the day, the IRI predicts significantly lower height and density. In particular, the difference in the height of the reconstructed layer and IRI layer is large during the 1100-1200 hrs, which coincides with the time of peak in equatorial vertical drift. Bottom side of the IRI predicted layer is remarkably thicker than the measured bottom side during this period. This suggest that the IRI probably used a temperature controlled profile over Dibrugarh which would cause larger thickness due to increase in scale height ($H = kT/mg$) and vertical expansion of the neutral distribution.

B. Comparison of vertical density profile with IRI

To investigate in detail the model and estimated profiles, we have compared the profile estimated for three different days in the same time period. Fig. 3 shows four reconstructed profiles for different times of the day and their comparison with the IRI predicted profile for ROCSAT-1 data. Equinoctial period is chosen to minimize seasonal effects in solstice conditions. The blue/green/black line represents the

bottom side electron density up to the peak of the F2-layer derived from ionosonde (CADI) data using POLAN for three different days with sane solar activity. The red colored line is the IRI 2012 predicted vertical electron density profile. The solar activity and magnetic activity during the period of measurements are shown by the F10.7 and Kp index respectively. It is evident that the measurements are for quiet period only and can be used to compare with model prediction. The IRI model predicts only the monthly mean profile and therefore three estimated profiles are shown. It is seen from this figure that the IRI model derived profiles underestimate the electron density at most times. Particularly at day time, the reconstructed profile differs significantly from the IRI profile which predicts the layer at lower heights than the measured bottom side profile. The model profile is thicker than the estimated bottom side profile. IRI underestimates the NmF2 at most hours except in post midnight period. The topside profile is similar to IRI but there are significant differences in bottom side.

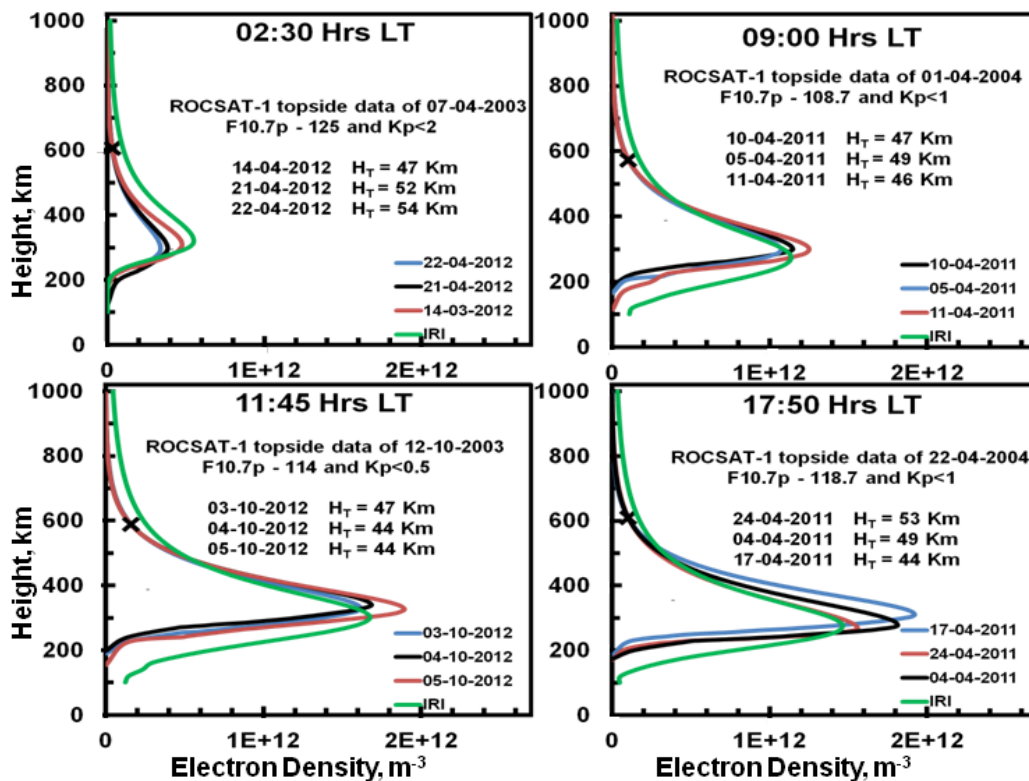


Fig. 3. Reconstructed vertical electron density profiles using ROCSAT-1 data. IRI predicted profile for the days of satellite measurements are also shown.

IV. CONCLUSIONS

In this work, bottom side electron density measured using CADI and topside in-situ electron density measurements made by ROCSAT-1 satellite are used to fit a α -Chapman function to derive the effective topside Chapman scale height. The topside density is

reconstructed from the scale height and the Chapman profile. The total vertical density profile is obtained by adding the bottomside provided by POLAN and the reconstructed topside. The reconstructed total electron density profiles are compared with IRI predicted profiles.

Following conclusions can be drawn
 -IRI model underestimates the peak density and the height of peak density of F2 layer at most times.
 -IRI predicts thicker bottom side F2 layer compared to the CADI-POLAN provided bottom side.

ACKNOWLEDGEMENT

The authors wish to express sincere thanks to ISRO for providing the funding for CADI and NOVATEL GPS receiver through its SSPS program. The authors are also indebted to the members of the Taiwanese satellite ROCSAT-1 project for the ion density data used in this analysis.

REFERENCES

- [1]. Belehaki, A., Jakowski, N., and Reinisch, B. (2003). Comparison of ionospheric ionization measurements over Athens over Athens using ground ionosonde and GPS derived TEC values, *Radio Sci.*, **38**(6), 1105, doi:10.1029/2003RS002868, 2003.
- [2]. Bhuyan, P.K., Chamua, M., Subrahmanyam, P., Garg, S.C. (2002). Diurnal, Seasonal and latitudinal variations of electron temperature measured by the SROSS C2 satellite at 500 km altitude and comparison with the IRI, *Annales Geophysicae*, **20**: 807–815.
- [3]. Booker, H. G. (1977). Fitting of multi-region ionospheric profiles of electron density by a single analytic function of height, *J. Atmos. Terr. Phys.*, **39**, 619–623, doi:10.1016/0021-9169(77)90072-1.
- [4]. Borgohain, A. and Bhuyan, P. K. (2010). Solar cycle variation of ion densities measured by SROSS C2 and FORMOSAT-1 over Indian low and equatorial latitudes, *J. Geophys Res*, Vol. **115**, A04309, doi:10.1029/2009JA014424, 2010.
- [5]. Davies, K. (1990). *Ionospheric Radio*. Peter Peregrinus Ltd., London.
- [6]. Di Giovanni, G. and Radicella, S. M. (1990). An analytical model of the electron density profile in the Ionosphere, *Adv. Space Res.*, **10**, 27–30, doi:10.1016/0273-1177(90)90301-F.
- [7]. Frederick J. Rich, Peter J. Sultan, and William J. Burke. (2003). The 27-day variations of plasma densities and temperatures in the topside ionosphere, *J. Geophys Res*, Vol. **108**, NO. A7, 1297, doi: 10.1029/2002JA009731, 2003.
- [8]. Hanson, W.B., Ortenburger, I.B. (1961). The coupling between the protonosphere and the normal F region. *J. Geophys Res.*, **66**, 1425–1435.
- [9]. Hargreaves, J. K. (1992). *The Solar-Terrestrial Environment*, pp. 1–420, Cambridge Univ. Press, New York, 1992.
- [10]. Horwitz, J.L., Comfort, R.H., Richards, P.G., Chappell, C.R., Chandler, M.O., Anderson, P., Hanson, W.B., Brace, L.H. (1990). Plasmasphere–ionosphere coupling: 2. Ion composition measurements at plasmaspheric and ionospheric altitudes and comparison with modelling results. *Journal of Geophysical Research*, **95**, 7949–7959.
- [11]. Huang, X., and Reinisch, B. W. (2001). Vertical electron content from ionograms in real time, *Radio Sci.*, **36**(2), 335–342, doi:10.1029/1999RS002409, 2001.
- [12]. Lei, J., Liu, L., Wan, W., Zhang, S.R. (2005). Variations of electron density based on long-term incoherent scatter radar and ionosonde measurements over Millstone Hill, *Radio Science*, Vol. **40**, RS2008, doi:10.1029/2004RS003106.
- [13]. Liu, L., W. Wan, and B. Ning. (2005). A study of the ionogram derived effective scale height around the ionospheric hmF2, *Ann. Geophys.*, **24**, 851–860, 2005.
- [14]. Liu, L., H. Le, W. Wan, M. P. Sulzer, J. Lei, and M.L. Zhang. (2007a). An analysis of the scale heights in the lower topside ionosphere based on the Arecibo incoherent scatter radar measurements, *J. Geophys. Res.*, **112**, A06307, doi:10.1029/2007JA012250,2007a
- [15]. Liu, L., Wan, W. Zhang, M. L. Ning, B. Zhang, S.-R. and Holt, J. M. (2007b). Variations of topside ionospheric scale heights over Millstone Hill during the 30-day incoherent scatter radar experiment, *Ann. Geophys.*, **25**, 2019–2027, 2007b.
- [16]. Liu, L., He, M., Wan, W. and Zhang, M.L. (2008). Topside ionospheric scale heights retrieved from Constellation Observing System for Meteorology, Ionosphere, and Climate radio occultation measurements, *J. Geophys. Res.*, **113**, A10304, doi:10.1029/2008JA013490,2008.
- [17]. Oyama, K.-I., Watanabe, S., Su, Y., Takahashi, T., and Hiro, K. (1996). Season, local time, and longitude Variations of electron Temperature at the height of - 600 km in the low latitude region. *Adv Space Res*. Vol. **18**, No. 6. pp. (6)269–(6)278, 1996.
- [18]. Rawer, K., D. Bilitza, and T. L. Gulyaeva. (1985). New formulas for IRI electron density profile in the topside and middle ionosphere, *Adv. Space Res.*, **5**(7), 3–12, doi:10.1016/0273-1177(85)90347-3,1985.
- [19]. Rawer, K. Synthesis of ionospheric electron density profiles with Epstein functions, *Adv. Space Res.*, **8**(4), 191–198, doi:10.1016/0273-1177(88)90239–6,1988.
- [20]. Reinisch, B. W., and X. Huang. (2001). Deducing topside profiles and total electron content from bottom side ionograms, *Adv. Space Res.*, **27**, 23–30. doi:10.1016/S0273-1177(00)0013608,
- [21]. Reinisch, B. W., Huang, X., Belehaki, A., Shi, J., Zhang, M., and Ilma, R. (2004). Modeling the IRI topside profile using scale height from ground- based ionosonde measurements, *Adv. Space Res.*, **34**, 2026–2031, doi:10.1016/j.asr.2004.06.012,.
- [22]. Rishbeth, H., and O. K. Garriott. (1969). *Introduction to Ionospheric Physics*, pp. 1–331, Academic, New York.
- [23]. Stankov, S. M., Jakowski, N., Heise, S., Muhtarov, P., Kutiev, I., and Warnant, R. (2003). A new method for reconstruction of the vertical electron density distribution in the upper ionosphere and plasmasphere, *J. Geophys. Res.*, **108**(A5), 1164, doi:10.1029/2002JA009570.
- [24]. Stankov, S. M., and Jakowski, N. (2006). Topside ionospheric scale height analysis and modelling based on radio occultation measurements, *J. Atmos. Sol. Terr. Phys.*, **68**, 134–162, doi:10.1016/j.jastp.2005.10.003.
- [25]. Titheridge, J. (1985). *Ionogram analysis with the generalized program POLAN*”, World Data Center Report, UAG-93, WDC-A-STP, Boulder, CO, 194 pp.
- [26]. Tulasi Ram, S., Su, S. Y., Liu, C. H., Reinisch, B. W., and McKinner, L. A. (2009). Topside ionospheric effective scale heights (HT) derived with ROCSAT-1 and ground-based ionosonde observations at equatorial and mid latitude stations, *J. Geophys. Res.*, **114**, A10309, doi:10.1029/2009JA014485, 2009.
- [27]. Venkatesh, K., Rama Rao, P. V. S., Saranya, P. L., Prasad, D. S. V. V. D. and Niranjana, K. (2011). Vertical electron density and topside effective scale height (HT) variations over the Indian equatorial and low latitude stations *Ann. Geophys.*, **29**, 1861–1872,2011.
- [28]. Zhang, M.L., Reinisch, B. W. Shi, J. S., Wu, S. and Wang, X. (2006). Diurnal and seasonal variation of the ionogram-derived scale height at the F2 peak, *Adv. Space Res.*, **37**, 967–971, doi:10.1016/j.asr.2006.02.004, 2006.